10.1071/EN19095_AC

Environmental Chemistry 2019, 16(7), 505-516

Supplementary Material

Emergent functional behaviour of humic substances perceived as complex labile aggregates of small organic molecules and oligomers

Elena A. Vialykh,[A,G] Dennis R. Salahub,[B,C] Gopal Achari,[D] Robert L. Cook[E] and Cooper H. Langford[A,F]

[A]Department of Chemistry, University of Calgary, 2500 University Dr. NW, Calgary, AB, Canada, T2N 1N4.

[B]Department of Chemistry, CMS – Centre for Molecular Simulation, IQST - Institute for Quantum Science and Technology and Quantum Alberta, University of Calgary, 2500 University Drive NW, Calgary, Alberta, Canada, T2N 1N4.

[C]College of Chemistry and Chemical Engineering, Henan University of Technology, 100 Lian Hua Street, High-Tech Development Zone, Zhengzhou 450001, China.

[D]Schulich School of Engineering, University of Calgary, 2500 University Dr. NW, Calgary, AB, Canada, T2N 1N4.

[E]Department of Chemistry, Louisiana State University, 307 Choppin Hall, Baton Rouge, LA 70803, USA.

[F]Deceased.

[G]Corresponding author. Email: elena.vialykh@ucalgary.ca

Table of Contents

Table S1. Chemical characteristics of three organic models created to perform computational modeling

SRFA-22 model (total number of atoms 513)						
N of molecules	Chemical formula	Carbonyl	Carboxyl	Aromatic	Heteroaliphatic	Aliphatic
2	$C_4H_4O_4$	0	2	2	0	0
3	$C_5H_8O_3$	1	1	0	0	3
3	$C_6H_{12}O_3$	0	1	0	1	4
2	$C_4H_6O_5$	0	2	0	1	1
1	$C_7H_6O_3$	0	1	6	0	0
1	$C_{10}H_{20}O_2$	0	1	0	0	9
1	$C_9H_6O_4$	0	0	9	0	0
1	$C_{16}H_{14}O_6$	2	0	12	2	0
2	$C_4H_6O_4$	0	2	0	0	2
3	$C_{10}H_{14}O_7$	0	2	0	5	3
1	$C_{16}H_{14}O_{10}$	1	4	6	0	5
2	$C_{17}H_{14}O_{11}$	2	4	6	0	5

SRFA-6 model (total number of atoms 550)							
N of molecules	Chemical formula	Carbonyl	Carboxyl	Aromatic	Acetal	Heteroaliphatic	Aliphatic
1	$C_{34}H_{38}O_{21}$	3	7	6	0	7	11
1	$C_{37}H_{44}O_{22}$	2	8	6	1	4	16
1	$C_{35}H_{43}O_{21}N$	3	6	6	3	5	12
1	$C_{33}H_{37}O_{16}N$	2	6	10	0	4	11
1	$C_{31}H_{30}O_{19}$	2	8	10	0	1	10
1	$C_{33}H_{35}O_{17}NS$	2	6	12	0	6	7

SRHA-6 model (total number of atoms 509)							
N of molecules	Chemical formula	Carbonyl	Carboxyl	Aromatic	Acetal	Heteroaliphatic	Aliphatic
2	$C_{33}H_{32}O_{19}$	2	4	12	1	4	8
1	$C_{38}H_{43}O_{19}N$	2	6	12	1	6	11
1	$C_{31}H_{31}O_{16}N$	2	5	12	0	4	8
1	$C_{31}H_{25}O_{16}N$	2	6	15	0	1	7
1	$C_{36}H_{31}O_{19}NS$	2	6	18	0	6	4

Table S2. Composition of standard IHSS samples of Suwannee River humic and fulvic acids ("IHSS | International Humic Substances Society")

Parameter	Humic acids	Fulvic acids
Elemental composition (mass %)		
C	52.55	52.44
O	42.53	42.20
H	4.40	4.31
N	1.19	0.72
S	0.58	0.44
Functional group content (meq g^{-1})		
-COOH	9.59	11.4
Phenolic	4.24	2.91
Structural composition (C, %)		
Carbonyl	8	7
Carboxyl	19	20
Aromatic	37	24
Acetal	9	5
Heteroaliphatic	7	11
Aliphatic	21	33

Text S1. Chemical characteristics of SRFA used to build a model.

The hypothetical structures of SRFA proposed by Leenheer et al.(1994) were designed by integrating state-of-the-art knowledge from analytical data on SRFA, including the following characteristics:

1. Number-average molecular weight.
2. Elemental contents corrected for moisture and ash contents:
   Carbon (C)
   Hydrogen (H)
   Oxygen (0)
   Nitrogen (N)
   Sulfur (S)
   Phosphorus (P)
3. Average molecular formula.
4. Average moles of unsaturation (ϕ).
5. Carbon distribution by type of carbon:
   Aliphatic
   H-C-0 (alcohol, ether, ester, acetal, ketal)
   0-C-O (acetal, ketal) plus aromatic
   Aromatic
   Phenols, phenolic esters, aromatic ethers
   Carboxyl plus ester
   Ketone
6. Hydrogen distribution:
   Exchangeable-hydrogen distribution by type of hydrogen:
   Carboxyl
   Phenol
   Alcohol
   Nonexchangeable hydrogen distribution by type of hydrogen:
   Isolated aliphatic
   H_3C-C=0, H_2C-C=0, H-C-C=0, H_3 -C-ϕ, H_2-C-ϕ, H-C-ϕ, H-C-O, H- ϕ
7. Oxygen distribution by type of oxygen:
   Carboxyl

Ester

Carboxyl+ester

Ketone

Phenol

Alcohol

Acetal and ketal

Ether

8. Amino acids

   Metal-binding sites, nitrogencontaining functional groups

   Metal-binding sites, sulfurcontaining functional groups

9. Organic free radicals
10. Metal-binding sites

Suwanee River fulvic and humic acids were of particular interest due to the following factors: i) they have been accepted as standard humic materials by the international scientific community, IHSS in particular, ii) there is a large body literature available, including extensive molecular level characterization, and iii) they are available to anyone in the international community at a very reasonable price

Text S2. Description of ReaxFF force field.

In 2001 van Duin et al. (2001) developed a new force field (ReaxFF). The main advantage of ReaxFF is its ability to simulate covalent bond formation and breaking, i.e. primary chemical reactions of organic molecules. The general equation used in ReaxFF is:

$$E_{system} = E_{bond} + E_{over} + E_{under} + E_{lp} + E_{val} + E_{tor} + E_{wdWaals} + E_{Coloumb} \quad (1)$$

It takes into account partial contributions to the total system potential energy (E_{system}) related to the bond (E_{bond}), over-coordination penalty (E_{over}) and under-coordination stability (E_{under}), lone pair (E_{lp}), valence angle (E_{val}) and torsion (E_{tor}), and non-bonding Coulombic ($E_{Coloumb}$) and van der Waals ($E_{wdWaals}$) energies, respectively (Russo and van Duin 2011).

The main assumption used in ReaxFF is that bond order (BO_{ij}) can be derived directly from interatomic distance (r_{ij}) according to equation (2):

$$BO'_{il} = \exp\left[p_{bo,1} * \left(\frac{r_{ij}}{r_0} \right)^{p_{bo,2}} \right] + \exp\left[p_{bo,3} * \left(\frac{r_{ij}^{\pi}}{r_0} \right)^{p_{bo,4}} \right] + \exp\left[p_{bo,5} * \left(\frac{r_{ij}^{\pi\pi}}{r_0} \right)^{p_{bo,6}} \right] \quad (2),$$

where r_o is the bonding equilibrium distance. Three exponential terms used in equation (2) describe: 1) the sigma bond ($p_{bo,1}$ and $p_{bo,2}$) which is unity below ~1.5 Å but negligible above ~2.5 Å; 2) the first pi bond ($p_{bo,3}$ and $p_{bo,4}$) which is unity below ~1.2 Å and negligible above ~1.75 Å, and 3) the second pi bond ($p_{bo.5}$ and $p_{bo,6}$) which is unity below ~1.0 Å and negligible above ~1.4 Å. As result a carbon-carbon bond has a maximum bond order of 3. For carbon-hydrogen and hydrogen-hydrogen bonds, only the sigma-bond contribution is considered, resulting in a maximum bond order of 1 (van Duin et al. 2001). The use of two main relationships, bond distance/ bond order on the one hand and bond order/ bond energy on the other, allows modeling of bond dissociation and formation with ReaxFF.

The terms E_{over}, E_{under}, E_{lp} are used to adjust bond order over-/under-coordination happening due to long-range interactions. When a carbon has a weak attraction/bond order with its second nearest

neighbor, hydrogen atoms, this type of bonding will cause unrealistic behavior while modeling intact molecules, and must be corrected. In other words when a carbon atom has a bond order of 4 or more, these types of long range interactions need to be negated and thus the small bond orders involving this carbon are significantly reduced to minimize their effects. Conversely, when a carbon atom has less than its optimal 4 bonds, these types of weak interactions should be allowed, so the weak bond orders are essentially unchanged. Consequently, these corrections allow accurate modeling of long-range radical attraction between atoms from different molecules as well as the realistic interactions between a radical site and its second nearest neighbors within the same molecule (Russo and van Duin 2011).

Since the bond orders are combined with functions of valence coordinates such as bond angles and torsion angles (equation 3) so that the energy contributions from bonding terms go to zero smoothly as bonds break.

$$E_{val} = \left[1 - \exp\left(\lambda * BO_1^3\right)\right] * \left[1 - \exp\left(\lambda * BO_2^3\right)\right] * \left\{k_a - k_b * \exp\left(-k_b * \left(\phi - \phi_0\right)^2\right)\right\} \qquad (3),$$

where BO_1 and BO_2 are the bond orders for each of the two bonds connecting the three atoms within an angle. λ is an angular parameter set to obtain agreement with quantum calculated values, k_a and k_b are the harmonic force constants that determine the depth and width of the angular potential, respectively, ϕ is the angle, and ϕ_0 is the equilibrium angle (Russo and van Duin 2011).

ReaxFF also allows the calculation of the polarization of charges within molecules (eq. 4):

$$\frac{\partial E}{\partial q_n} = \chi_n + 2 * q_n * \eta_n + C * \sum_{j=1} \frac{q_j}{\left\{r_{nj}^3 + \left(1/\gamma_{nj}\right)^3\right\}^{1/3}}, \qquad (4).$$

In equation (4) χ_n is the electronegativity and η_n is the hardness of element n and γ_{nj} is a shielding parameter between atoms n and j. The charge values are dependent on the system geometry and determined for each time step of the simulation (Russo and van Duin 2011).

The van der Waals and Coulomb forces are included from the beginning and calculated (eq. 5)

between every atom pair which allows the description of non-bonded interactions between all atoms.

$$E_{Coulomb} = C * \left[\frac{q_i * q_j}{\left\{ r_{ij}^3 + \left(1/\gamma_{ij} \right)^3 \right\}^{1/3}} \right] \quad (5),$$

where q_i and q_j are the charges of the two atoms, r_{ij} is the interatomic distance and C is the electric constant, and γ_{ij} is the shielding parameter between atoms i and j (Russo and van Duin 2011).

Parameters for the dissociation and reaction curves are derived from quantum chemical calculations, thus ReaxFF allows molecular dynamics simulations of large scale reactive chemical systems (1000s of atoms) with resulting accuracy similar to quantum mechanically based methods, yet ReaxFF is about 100 times faster (van Duin et al. 2001).

Table S3. Characteristics of three organic models after MD simulations at 300 K in vacuum.

	SRFA-22	SRFA-6	SRHA-6
Number of H-bonds	21±2	17±2	14±1
Change in potential energy of the system*, kJ mol^{-1}	-790	-949	-493

* The value determined as the difference between potential energy of the system minimized right after packing and average potential energy of the system during last 0.1 ns of MD simulations.

Figure S1. Temperature profile of MD simulations carried out to achieve interactions occurred at higher activation energy or reactions required longer time to occur.

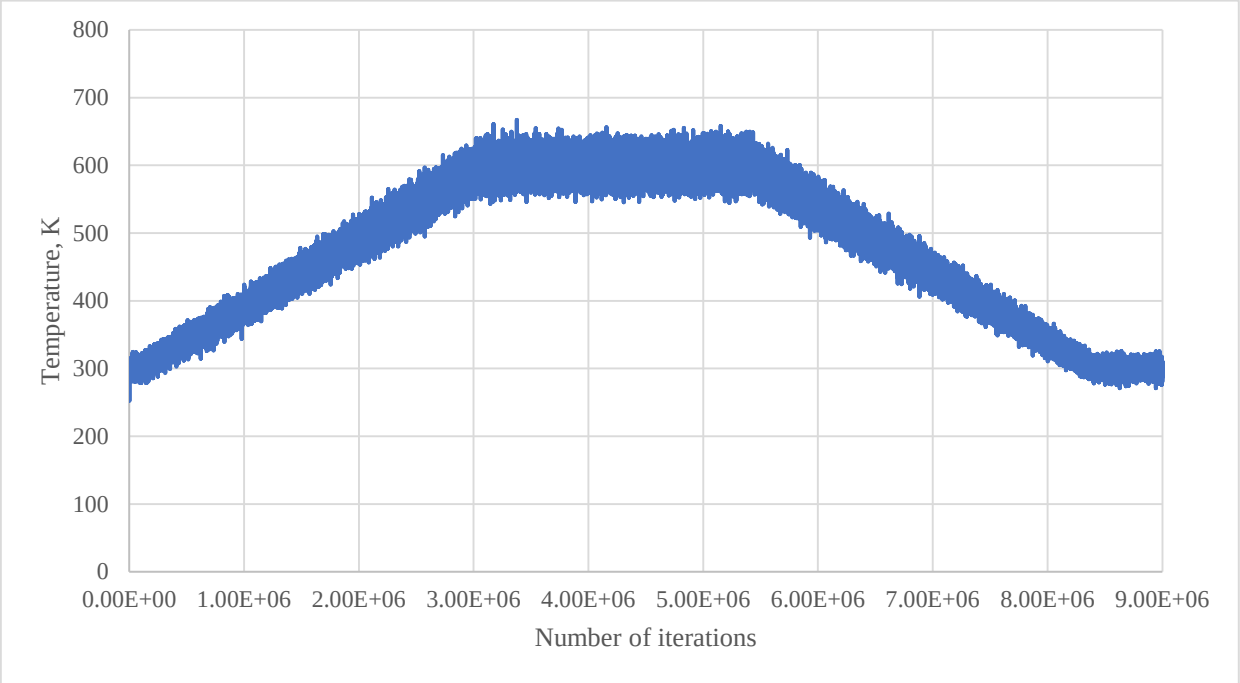

Figure S2. Formation of π-stacking cluster in organic models' aggregates formed in vacuum conditions after temperature increase to 600 K followed by cooling down the systems to 300 K: a) two molecular fragments with aromatic rings are involved in formation of π-stacking cluster in SRFA-22 model; b) four aromatic rings are involved in formation of π-stacking cluster in SRFA-6 model.

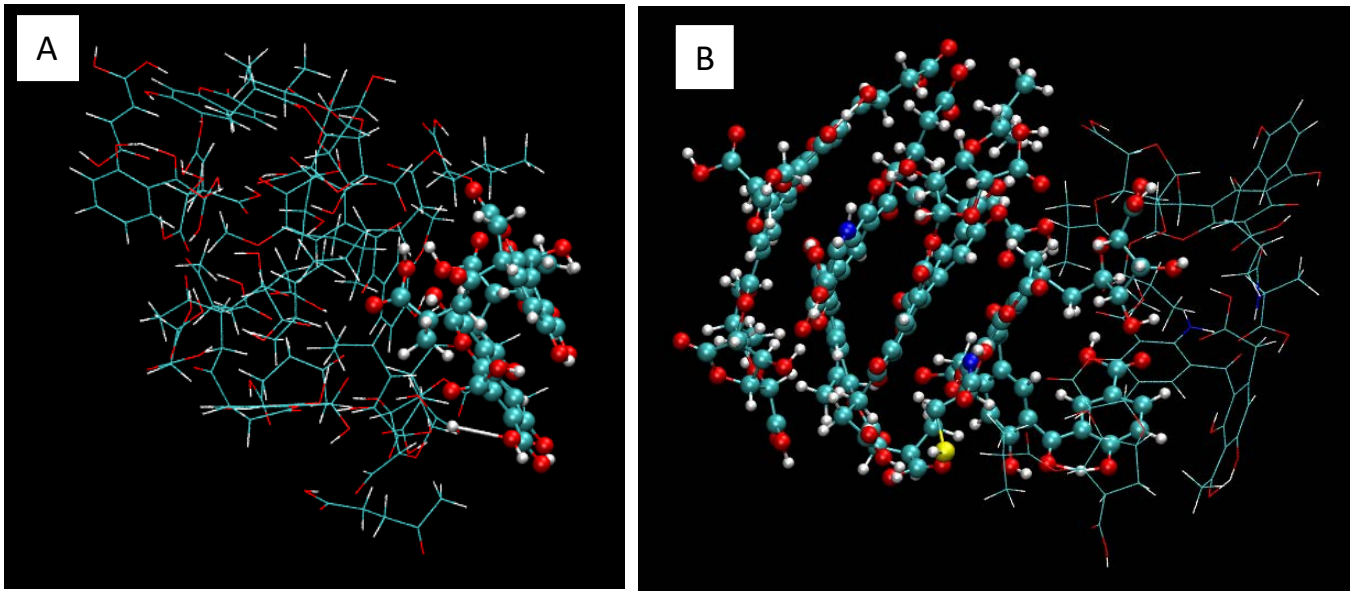

Figure S3. Chemical structures of molecular fragments before (A, B) and after (C, D) MD simulations, where proton transfer interactions occurred. A and C are structures of molecular fragment in SRFA-22 model and B and D are structures of molecular fragment in SRHA-6 model.

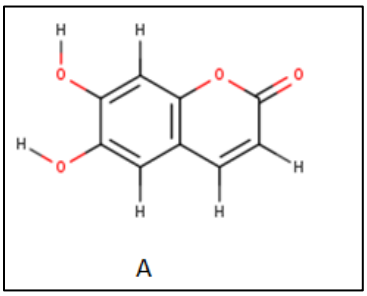

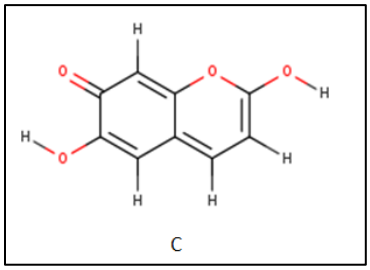

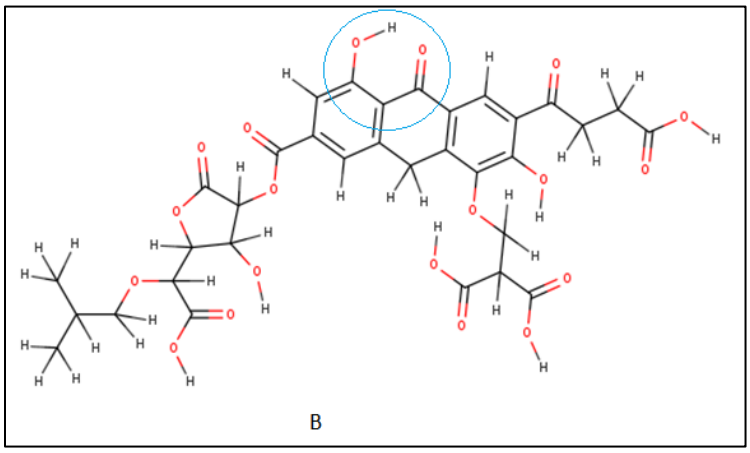

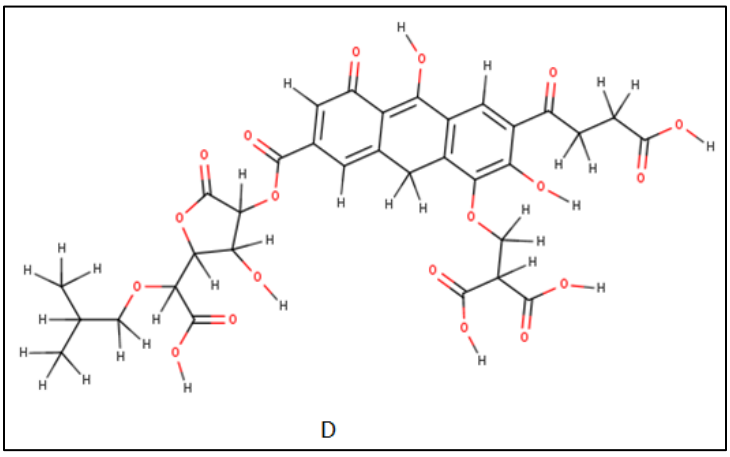

Figure S4. Cu^{2+} ion binding in SRFA-6 model: (A) is initial input structure; (B) is the metal-organic ligand complex formed over MD simulations.

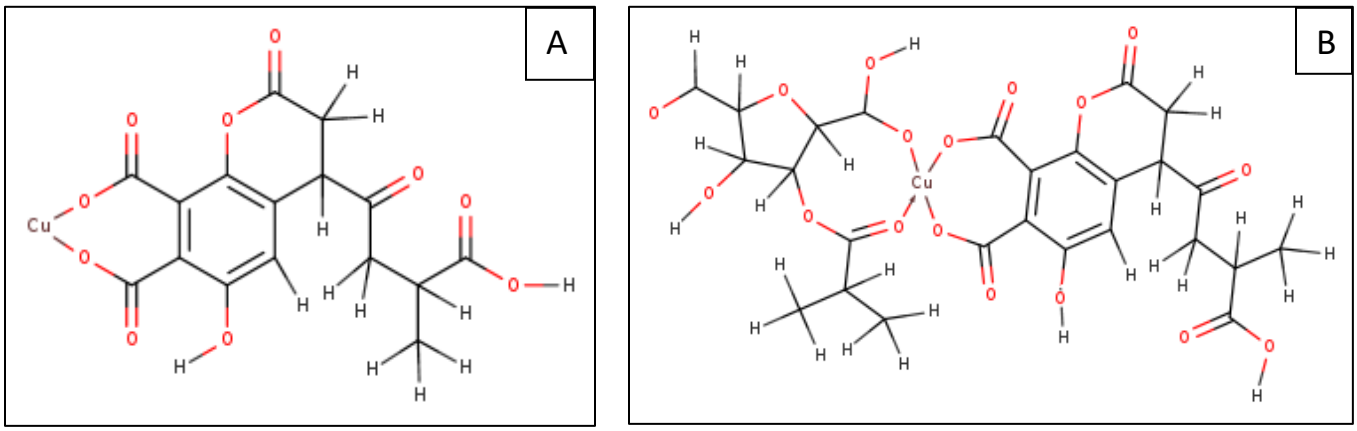

Text S3. The charge redistribution in organic models.

The charge distribution between molecules and atoms in all three systems was perturbed by the addition of the Cu^{2+} ion. The charge of the Cu ion was reduced to +1.15±0.03, +1.13±0.03 and +1.15±0.03 for SRFA-22, SRFA-6 and SRHA-6, respectively. The positive charge lost from the Cu ion was redistributed throughout each of the three systems in a complex manner with the total charge of each of the molecules in each of the systems changing (Table S4). Overall, molecules with a dominantly hydrocarbon structure became more positively charged, whereas molecules with a large number of carboxyl groups became more negatively charged. These trends are most obvious in SRFA-22, where molecular fragments can be easily distinguished by this property, for SRFA-6 and SRHA-6 the changes in molecular charge is not that obvious as each fragment contains both hydrocarbon and carboxylic parts. These findings show that electron shuttling, an emergent property, within HS and NOM as whole is in all likelihood a very complex process and not the simple transfer of electrons through a conjugated system or stacked aromatic moieties and requires additional examination.

Table S4. Molecular charge of each molecule in SRFA and SRHA models with Cu^{2+} ion before and after MD simulations.

SFRA-22				
#	formula	Molecular mass, g mol^{-1}	Initial molecular charge*	Molecular charge after MD simulations*
1	$C_4H_4O_4$	116.03	-0.160	-0.399
2	$C_4H_4O_4$	116.03	-0.075	-0.468
3	$C_5H_8O_3$	116.06	0.028	-0.093
4	$C_5H_8O_3$	116.06	0.019	0.019
5	$C_5H_8O_3$	116.06	0.019	-0.007
6	$C_6H_{12}O_3$	132.09	0.166	0.273
7	$C_6H_{12}O_3$	132.09	0.178	0.576
8	$C_6H_{12}O_3$	132.09	0.110	0.170
9	$C_4H_6O_5$	134.04	-0.107	-0.391
10	$C_4H_6O_5$	134.04	-0.071	-0.276
11	$C_7H_6O_3$	138.05	0.062	-0.392
12	$C_{10}H_{20}O_2$	172.16	0.365	1.262
13	$C_9H_6O_4$	178.04	-0.136	0.182
14	$C_{16}H_{14}O_6$	302.11	0.245	0.400
15	$C_4H_6O_4$	118.04	-0.045	-0.060
16	$C_4H_6O_4$	118.04	-0.026	0.0004
17	$C_{10}H_{14}O_7$	246.11	-0.017	-0.018
18	$C_{10}H_{14}O_7$	246.11	0.113	0.131
19	$C_{10}H_{14}O_7$	246.11	-0.016	0.355
20	$C_{16}H_{12}O_{10}Cu$	427.63	-0.115	
21	$C_{17}H_{14}O_{11}$	394.10	-0.267	-0.537
22	$C_{17}H_{14}O_{11}$	394.10	-0.269	-0.727
SFRA-6				
1	$C_{35}H_{43}O_{21}N$	813.32	0.167	-0.056
2	$C_{37}H_{44}O_{22}$	840.33	-0.116	-0.034
3	$C_{34}H_{36}O_{21}Cu$	843.81	0.014	
4	$C_{33}H_{35}O_{17}NS$	749.32	0.058	
5	$C_{33}H_{37}O_{16}N$	703.28	0.0015	0.959
6	$C_{31}H_{30}O_{19}$	706.22	-0.124	0.155
SRHA-6				
1	$C_{33}H_{32}O_{19}$	732.24	-0.132	-0.050
2	$C_{38}H_{43}O_{19}N$	817.33	0.140	0.207
3	$C_{36}H_{31}O_{19}NS$	813.29	-0.014	-0.016
4	$C_{31}H_{31}O_{16}N$	673.23	-0.0011	-0.140

5	$C_{31}H_{25}O_{16}N$	667.18	-0.051	
6	$C_{33}H_{30}O_{19}Cu$	793.77	0.058	

* SD varied between ±(0.005÷0.01)

Table S5. The change in number of hydrogen bonds after MD simulations of dissolution process.

	SRFA-22			
	Without	Benzene	Phenol	Toluene
Initial	21±2	17±2	22±2	21±2
After heating	7±1	6±1	5±0.5	7±1
After cooling	7±1	8±1	5±0.5	9±1
	SRFA-6			
Initial	16±2	15±1	17±2	16±2
After heating	11±1	10±1	11±1	12±1
After cooling	10±1	9±1	10±1	11±1
	SRHA-6			
Initial	12±1	9±1	13±1	11±1
After heating	8±1	8±1	10±1	9±1
After cooling	7±1	6±1	9±1	7±1

Table S6. Change in energy (kJ mol^{-1}) of the HS models calculated as a difference between potential energy of each model before and after dissolution process.

	SRFA-22	SRFA-6	SRHA-6	Average change for three HS models with specific contaminant
Benzene	1688	900	548	1046
Toluene	1699	971	883	1184
Phenol	1891	920	920	1243
Without contaminant	1841	866	732	1146
Average change for each HS model	1782	916	770	

Table S7. The change of hydrophilic/hydrophobic surfaces (% of initial value, i.e. surface of the aggregates formed in vacuum) and total surface (calculated as a sum of hydrophobic and hydrophilic, $Å^2$) of HS models after dissolution process.

	Without contaminant	Phenol	Toluene	Benzene
	Hydrophilic surface area			
SRFA-22	204.6	207.1	175.3	201.6
SRFA-6	74.8	79.2	79.2	56.7
SRHA-6	75.3	79.7	78.9	47.4
Hydrophobic surface area				
SRFA-22	-3.0	4.5	1.4	2.7
SRFA-6	-3.0	-4.3	-2.2	0.0
SRHA-6	-18.9	2.4	-10.5	-15.2
Total surface area				
SRFA-22	2620	2840	2730	2650
SRFA-6	2270	2190	2170	1900
SRHA-6	2110	2170	2120	1960

References (Supplementary materials)

van Duin, A.C.T., Dasgupta, S., Lorant, F., Goddard, W.A., 2001. ReaxFF: A Reactive Force Field for Hydrocarbons. *J. Phys. Chem. A* **105**, 9396–9409. https://doi.org/10.1021/jp004368u

IHSS | International Humic Substances Society. URL http://humic-substances.org/ (accessed 12.11.17).

Leenheer, J.A., McKnight, D.M., Thurman, E.M., MacCarthy, P., 1994. Structural Components and Proposed Structural Models of Fulvic Acid from the Suwannee River. In 'Humic Substances in the Suwannee River, Georgia: Interactions, Properties, and Proposed Structures' 'US Geol. Serv., No 87-557' (Eds. Averett, R.C., Leenheer, J.A., McKnight, D.M., Thorn, K.A.).

Russo, M.F., van Duin, A.C.T., 2011. Atomistic-scale simulations of chemical reactions: Bridging from quantum chemistry to engineering. *Nucl. Instrum. Methods Phys. Res. Sect. B Beam Interact. Mater. At.* **269**, 1549–1554. https://doi.org/10.1016/j.nimb.2010.12.053